Lifetime and Distortion Optimization With Joint Source/Channel Rate Adaptation and Network Coding-Based Error Control in Wireless Video Sensor Networks

Junni Zou, *Member, IEEE*, Hongkai Xiong, *Senior Member, IEEE*, Chenglin Li, Ruifeng Zhang, *Member, IEEE*, and Zhihai He, *Senior Member, IEEE*

Abstract—In this paper, we study joint performance optimization on network lifetime and video distortion for an energy-constrained wireless video sensor network (WVSN). To seek an appropriate tradeoff between maximum network lifetime and minimum video distortion, a framework for joint source/channel rate adaptation is proposed, where the video encoding rate, link rate, and power consumption are jointly considered, formulating a weighted convex optimization problem. In the context of lossy wireless channels, an efficient error control scheme that couples network coding and multipath routing is explored. Moreover, an integrated power consumption model, including power dissipation on video compression, error control, and data communication, is specifically developed for the video sensor node. By primal decomposition, the original problem is decomposed into a two-level optimization procedure, with the high-level procedure for source adaptation (source rate optimization) and the low-level procedure for channel adaptation (network resource allocation). Finally, a fully decentralized iterative algorithm is developed to resolve the target optimization problem. Extensive simulation results evaluate the convergence performance of the proposed algorithm and demonstrate the best tradeoff performance.

Index Terms—Lifetime, power–rate–distortion (P-R-D), resource allocation, wireless video sensor networks (WVSNs).

I. INTRODUCTION

WIRELESS video sensor networks (WVSNs) are capable of capturing and processing visual information and delivering them to the sink over wireless channels [1]. In typical scenarios, such as target tracking and video surveillance,

a WVSN is supposed to support high data rates and provide high-quality video. High data rates necessitate a huge power consumption at the video sensor. However, battery-powered video sensors are often deployed in remote and unreachable locations, where battery replacement is impossible. Hence, there is an inherent tradeoff between using minimum power and achieving the highest video quality. The focus of this paper is on the design of adaptive power consumption, source coding rate, transmission rate, and multipath coding, achieving joint performance optimization on network lifetime and video distortion.

Over the past few years, a variety of power control, rate allocation, scheduling, and routing schemes have been proposed to maximize the lifetime of wireless sensor networks [2]–[7]. For instance, distributed algorithms for maximum lifetime routing have been studied in [2] and [3]. Wang *et al.* [4] investigated a cross-layer design approach for minimizing the energy consumption of a multiple-source and single-sink wireless sensor network. Lifetime optimization with joint power and rate control in interference-limited ad hoc networks has been considered in [5] and [6]. In [7], the authors exploited the interaction between network lifetime maximization and fair rate allocation. The power consumption model adopted in the foregoing literature is constructed on the basis of conventional sensor networks, where the data processing function at the sensor node is very simple, and the corresponding power consumption is assumed to be negligible. In WVSNs, the raw video of high rate is required to be compressed before being injected onto the channel. In this case, the energy utilized in video compression is significant and cannot be neglected anymore.

In our previous work [1], a power–rate–distortion (P-R-D) analytical model has been developed to characterize the relationship between power consumption of video encoding and its rate–distortion performance. Following this model, He *et al.* [8] proposed a distributed algorithm for maximizing the network lifetime of WVSNs. The scenario they considered is very simple, where the channel capacity is assumed unlimited, and the quality required for the reconstructed video is prescribed. When the video quality and the network lifetime concurrently become the targets, the cases would be more complicated and paradoxical since the video quality can be improved at the price

of the network lifetime, and *vice versa*. How to establish an appropriate tradeoff between these two conflicting properties has remained vastly unexplored in WVSNs.

Rate/channel adaptation has been proven as an effective means of enhancing the wireless network efficiency [9]–[11]. In channel adaptation, the data being communicated are considered to be generic and, thus, are generally encoded at the source with fixed rates. A combination of flexible channel adaptation with predetermined source rate is hard to fully utilize network resources. When the source rate exceeds the instantaneous channel capacity, network congestion would occur and could never be prevented by any rate adaptation scheme. On the contrary, the channel would be underutilized. The authors of [12] envisaged the nature of source data and proposed adaptive source encoding rates to satisfy the distortion constraints. However, their approach addressed the lifetime maximization problem for a single-hop wireless system. In this paper, we present a joint source/channel rate adaptation framework for multihop multipath WVSNs. It allows both the source rate and the transmission rate to vary with both channel conditions and distortion requirements.

Quality degradation arising from packet loss is quite challenging for wireless video transmission. Automatic repeat request adopts a feedback and retransmission scheme that is not suitable for delay-sensitive video applications [13]. Packet-level forward error correction (e.g., Reed–Solomon erasure (RSE) code [14]), which deals with erasures instead of bit errors, introduces check packets that require extra energy consumption. Recently, the combination of network coding with multipath routing (also referred to as multipath network coding) has emerged as a promising technique for reliable communication [15]–[17]. Most of the previous studies in this area focused on code design and parameter selection to guarantee successful decoding at the destination [18]. To the best of our knowledge, the power consumption behavior of network coding has not been investigated in the literature. In this paper, we develop a generalized power consumption model for network coding. Based on this model, the power consumed on multipath network coding could be incorporated with source coding and data communication power dissipation, forming an integrated power consumption model for the video sensor node.

The motivation of this paper is to address a joint performance optimization of network lifetime and video quality for energy-constrained WVSNs. To seek an optimal tradeoff between maximum network lifetime and minimum video distortion, we consider joint video encoding rate, aggregate power consumption, along with link rate allocation, formulating a weighted constrained convex optimization problem. Within the context of lossy wireless channels, an efficient error control scheme that couples network coding and multipath routing is explored. By primal decomposition, the original problem is decomposed into a two-level optimization procedure, with the high-level procedure for source adaptation and the low-level procedure for channel adaptation. Using the Lagrange dual approach, the low-level procedure is further decoupled into three subproblems: 1) rate control problem; 2) distortion control problem; and 3) energy conservation problem, which are solved separately and coordinated by Lagrange multipliers. Finally, a fully decentralized iterative algorithm is developed to solve the target optimization problem.

Compared with existing lifetime optimization approaches, the proposed algorithm is specifically developed for WVSNs and has the following major advantages:

1) Distributed joint optimization of network lifetime and video distortion. The previous work on performance optimization for a wireless sensor network mostly focused on extending the lifetime of the network. In WVSNs, not only the network lifetime but the video distortion is the major concern as well. We formulate the joint optimization of these two conflicting objectives as a weighted convex problem and propose a distributed algorithm with low communication overhead to resolve it.
2) Joint source/channel rate adaptation. To increase the resource utilization, we propose a framework for joint source/channel rate adaptation. The channel adaptation (network resource allocation) is achieved by solving rate control, distortion control, and energy conservation subproblems at individual sensor nodes and wireless links. Based on the resource allocation results in channel adaptation, each video source independently performs source adaptation (source rate optimization) by solving a localized optimization problem.
3) Source coding, data communication, and error control integrated power consumption model. Unlike the power consumption model of a conventional wireless sensor network, we consider power dissipation on video compression, multipath network coding-based error control, as well as data communication, establishing an integrated power consumption model for the video sensor node.

The rest of this paper is organized as follows: The network model and related specifications are presented in Section II. In Section III, the network coding-based error control scheme and its power consumption model are developed. In Section IV, we formulate the tradeoff problem of maximizing network lifetime and minimizing video distortion as a weighted convex optimization problem. A decentralized algorithm for joint rate allocation, distortion control, and energy conservation is proposed. We also prove the convergence of the iterative algorithm for updating the network lifetime and discuss an efficient implementation scheme. Experimental results are presented in Section V. Finally, we summarize this paper in Section VI.

II. SYSTEM MODELING

A. Network Model

A WVSN can be modeled as a directed graph $G(V, E)$, where V is the set of network nodes, and E is the set of directed links between nodes. The set V consists of two disjoint subsets S and T representing video sensor nodes and sink node, respectively. Video sensor nodes perform video capturing, video encoding, and packet routing. Sink nodes are remote control units or human interface devices acting as destinations of the WVSN. The transmission between each source–sink pair is called a session in this paper. All the sensor nodes have a maximum transmission range $d_{\max}$. A directed link $(i, j) \in E$
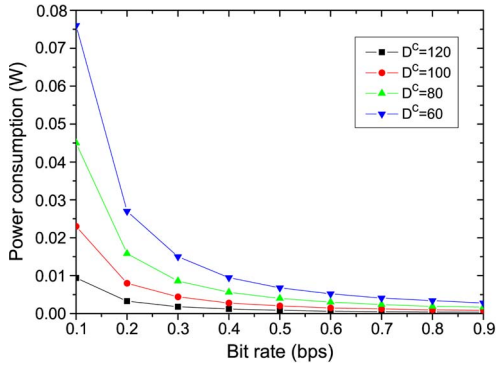
Fig. 1.   Relationship of video encoding power, rate, and distortion.

exists between nodes i and j if their distance d_{ij} satisfies $d_{ij} \leq d_{\max}$.

Suppose that there exist multiple alternative paths $J(s)$ between sensor node s and the sink node. Each node s is associated with a matrix H^s to reflect the relationship between its path and related links. Let $H_{ij}^{sm} = 1$ if path $m \in J(s)$ of sensor node s uses link (i, j), or else $H_{ij}^{sm} = 0$.

B. P-R-D Model

In video communication over lossy channels, the end-to-end distortion D is divided into two parts: 1) source coding distortion D^c caused by video compression and 2) transmission distortion D^t arising from channel errors. Since the encoding and transmission errors are generally uncorrelated, we have

$$D = D^c + D^t. \qquad (1)$$

This distortion model is proposed in [19]. Thereafter, it is widely used to estimate the end-to-end distortion in the literature [1], [20]. An analytic P-R-D model has already been developed in [1]. It characterizes the relationship of video coding power consumption P, source rate R, and its distortion D^c as

$$D^c(R, P) = \sigma^2 e^{-\gamma \cdot R \cdot P^{\frac{2}{3}}} \qquad (2)$$

where σ^2 is the average input variance, and γ is a model parameter related to the encoding efficiency.

Fig. 1 plots the encoding distortion D^c, measured in mean square error (MSE), as a function of source rate R and encoding power P. Clearly, a given encoding distortion can be guaranteed by controlling both the source rate and the encoding power. If we decrease the encoding power P or the source rate R, then the distortion D^c increases for the sake of insufficient compression power. On the other hand, if we increase the encoding power P, then the power used for transmission decreases, which also results in the increase of the distortion D^c. Further, if we simply adjust the encoding power or the source rate to a very low or very high level, then the encoding distortion will become large. Meanwhile, the total power consumed at the sensor node will increase fast [1]. Thus, an optimal allocation of R and P should be maintained to save the power consumption and control the video distortion.

C. Channel Interference Constraint

When a standard medium access control (MAC) protocol, e.g., IEEE 802.11, is adopted to coordinate the sensors' access to a shared channel, the communication activities among the links are no longer independent. Suppose any link originating from node k will interfere with link (i, j) if $d_{kj} < (1 + \Delta)d_{ij}$ or $d_{ki} < (1 + \Delta)d_{ij}$. Here, $\Delta \geq 0$ specifies the interference range. In other words, when node i is communicating with node j, any node whose distance to i or j is less than $(1 + \Delta)$ times that between i and j has to keep quiet. In addition, defining $\Psi(i, j)$ for each link $(i, j) \in E$ as the cluster of links that cannot transmit as long as link (i, j) is active, then the wireless network channel interference constraint can be defined as [21]

$$\sum_{s \in S} f_{ij}^s + \sum_{s \in S} \sum_{(p,q) \in \Psi(i,j)} f_{pq}^s \leq C \qquad (3)$$

where f_{ij}^s is the transmission rate of session s over link (i, j), f_{pq}^s is the transmission rate of session s along link $(p, q) \in \Psi(i, j)$ that would interfere with link (i, j), and C represents the maximum rate supported by the wireless shared medium.

III. NETWORK CODING-BASED ERROR CONTROL AND ITS POWER CONSUMPTION

A. Multipath Network Coding Scheme

Transmission errors, such as packet loss and packet corruption, frequently happen over wireless fading channels. To improve the reliability and reduce the transmission distortion D^t, we now present an efficient error control scheme based on multipath network coding.

Define the stream from its source to the sink as a separate session. Hence, the video data gathering in the sensor network is accomplished through multiple independent unicast sessions. Suppose that the original stream at the source is divided into generations [22], with each generation containing h packets denoted as $X_1, X_2, \ldots, X_h$. Using random linear coding, each outgoing packet Y_i is a linear combination of these original packets, namely

$$Y_i = \sum_{j=1}^{h} g_{ij} \cdot X_j \qquad (4)$$

where the set of coefficients $\mathbf{g} = [g_{i1}, \ldots, g_{ih}]$, which is also called the global encoding vector, is randomly picked from field $GF(2^q)$. Since network coding across different generations may increase the processing delay and computational complexity, we limit coding operations within the same generation. Consequently, packets of each generation can be decoded independently at the sink.

At the source node, the original packets are coded together before being injected on the outgoing links. With a multipath routing protocol (e.g., traditional disjoint multipath mechanism [23]), the coded streams traverse through multiple paths toward the sink node. A relay sensor, helping forward packets for other sensors, stores incoming packets into its buffer for a certain period. Packets that belong to the same generation but from different paths can be further combined at the relay sensor to

increase the information diversity. When the sink receives h packets with linearly independent global encoding vectors, it can perform decoding by Gaussian elimination and recover the original packets.

For any video session s originating from sensor s, suppose that there are, respectively, $A_{ij}^s(\tau)$ and $B_{ij}^s(\tau)$ coded packets injected and received on link (i, j) at a time period of τ. If the packet loss rate on link (i, j) is p_{ij}, then we have $B_{ij}^s(\tau) = \sum_{k=1} A_{ij}^s(\tau) Z_k$, where Z_k is a Bernoulli random variable with $\Pr(Z_k = 0) = p_{ij}$. If the packets are injected and received on link (i, j) at the average rates of f_{ij}^s and x_{ij}^s, then we have [17]

$$
\begin{aligned}
x_{ij}^s &= \lim_{\tau \to \infty} \frac{B_{ij}^s(\tau)}{\tau} = \lim_{\tau \to \infty} \frac{\sum_{k=1}^{A_{ij}^s(\tau)} Z_k}{\tau} \\
&= \lim_{\tau \to \infty} \frac{\sum_{k=1}^{A_{ij}^s(\tau)} Z_k}{A_{ij}^s(\tau)} \cdot \frac{A_{ij}^s(\tau)}{\tau} = (1 - p_{ij}) \cdot f_{ij}^s.
\end{aligned} \quad (5)
$$

It is mentioned that the packet loss rate p_{ij} of link i, j can be estimated at nodes i and j if real-time transport protocol/real-time transport control protocol is employed at each node.

In the preceding formulation, the linear correlation among different encoding vectors is not taken into account. Therefore, the coded data received at each node are decodable as long as the flows injected and received on any link (i, j) are equivalent. Since there exists a small probability of linear correlation among the encoding vectors, we introduce a slack factor κ and let

$$
\kappa \cdot x_{ij}^s = (1 - p_{ij}) \cdot f_{ij}^s \quad (6)
$$

where $\kappa > 1$. This way, for each link (i, j), the injected flow rate f_{ij}^s would be larger than the received flow rate x_{ij}^s, with their difference offsetting the linear correlation.

B. Integrated Power Consumption Model

1) Power Consumption Model on Data Communication: In our design, the total power of a video sensor is mainly used for four important processes: 1) video compression; 2) data transmission; 3) data reception; and 4) multipath network coding. The video compression power consumption can be calculated by the P-R-D model. Based on the power consumption model extensively used in wireless sensor networks [7], [8], the transmission power consumption at node i can be defined as

$$
P_i^t = \epsilon_{ij} \cdot \sum_{s \in S} \sum_{j:(i,j) \in E} f_{ij}^s \quad (7)
$$

where $\epsilon_{ij} = \theta + \eta \cdot (d_{ij})^\alpha$ is the transmission energy consumption cost of link (i, j), θ is the energy cost of transmit electronics, η is a coefficient term corresponding to the energy cost of transmit amplifier, and α is the path loss factor.

The reception power consumption at a node i can be formulated as

$$
P_i^r = \xi \cdot \sum_{s \in S} \sum_{j:(j,i) \in E} f_{ji}^s \quad (8)
$$

where ξ is the energy consumption cost of the radio receiver.

2) Power Consumption Model of Network Coding: Assume that each packet consists of L bits. Letting $GF(2^q)$ represent the Galois field, then each q consecutive bits of a packet can be viewed as a symbol over field $GF(2^q)$. In addition, assuming that L is a multiple of q, then each packet is composed of a vector of L/q symbols. To obtain a coded packet Y_i defined in (4), it is observed that $h \cdot (L/q)$ times of multiplication and $(h - 1) \cdot (L/q)$ times of addition should be performed in $GF(2^q)$. Although some practical coding methods have recently been employed in wireless protocols (e.g., XOR coding in a MAC extension known as COPE [24]), we just develop a generalized model for theoretical network coding, upon which simplified versions can easily be obtained.

Let $\varepsilon_* \cdot q^3$ and $\varepsilon_+ \cdot q$ denote the energy consumption per q-bit multiplication and addition, respectively. Here, ε_* and ε_+ are energy consumption cost determined by specific complementary metal–oxide-semiconductor (CMOS) technology [25]. Thus, the energy consumed on packet Y_i can be formulated as

$$
\varphi^p = \varepsilon_* \cdot q^3 \cdot h \cdot (L/q) + \varepsilon_+ \cdot q \cdot (h - 1) \cdot (L/q). \quad (9)
$$

The unit power consumption cost is then given by

$$
\begin{aligned}
\varphi &= \varepsilon_* \cdot q^3 \cdot h \cdot (L/q) + \varepsilon_+ \cdot q \cdot (h - 1) \cdot (L/q) L \\
&= \varepsilon_* \cdot q^2 \cdot h + \varepsilon_+ \cdot (h - 1).
\end{aligned} \quad (10)
$$

Correspondingly, the network coding power consumption at node i is formulated as

$$
P_i^{nc} = \varphi \cdot \sum_{s \in S} \sum_{j:(j,i) \in E} x_{ji}^s. \quad (11)
$$

From (10), we can find that the power consumption cost is mainly determined by the Galois field size q and the generation size h. It would be true that the encoding vectors are linearly independent if they are generated randomly from a Galois field of sufficient size. The field size q, however, cannot be too large, since not only the cost of the power consumption but the complexity of the code also grows with the field size. It has been proven that if q is 8, then the probability that the matrix of the encoding vectors received at the sink node has full rank is at least 99.6% [22].

Fig. 2 shows the relationship of generation size h and power consumption cost, where we have $\varepsilon_* = 3.7 \times 10^{-5}$ (W/MHz) and $\varepsilon_+ = 3.3 \times 10^{-5}$ (W/MHz), measured on 0.18-μm 2.5-V CMOS platform, and the arithmetic circuit is simulated by the gate-level simulator mean estimator of density [25]. It is observed that the power consumption cost is approximately in proportion to the generation size h. This implies that h should not be too large.

Fig. 3 shows the impact of h on the communication overhead of network coding, i.e., the overhead of transmitting extra h encoding vectors in each packet. Here, an average packet is supposed to be about 1400 B for realistic Internet settings. As shown in Fig. 3, the communication overhead increases fast with the generation size h and the field size q. With relatively small h and q (e.g., $h = 50$ and $q = 8$), the overhead is tolerant and is only about 3%.
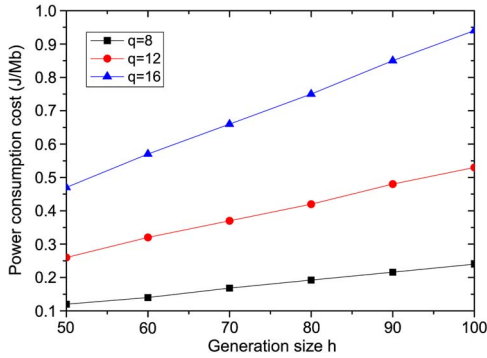
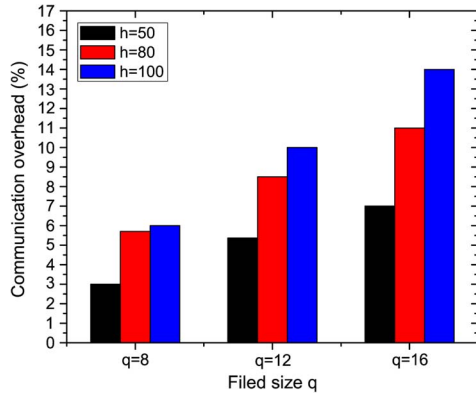Fig. 2.   Power consumption cost versus generation size.

Fig. 3.   Communication overhead versus generation size and field size.

Based on the preceding analysis, the total power dissipation at a sensor node i is given by

$$
\begin{aligned}
P_i &= P_i^c + P_i^t + P_i^r + P_i^{nc} \\
&= P_i^c + \epsilon_{ij} \cdot \sum_{s \in S} \sum_{j:(i,j) \in E} f_{ij}^s \\
&\quad + \xi \cdot \sum_{s \in S} \sum_{j:(j,i) \in E} f_{ji}^s + \varphi \cdot \sum_{s \in S} \sum_{j:(j,i) \in E} x_{ji}^s \quad (12)
\end{aligned}
$$

where P_i^c represents the video encoding power at node i.

IV. PROBLEM STATEMENT

A. Optimization Problem

For an energy-constrained wireless sensor network, one major concern is how to optimize the energy utilization and prolong the lifetime of the network. Supposing that each sensor i has an initial energy E_i and a lifetime of $T_i = E_i/P_i$, we define the lifetime of the network as $T_{\text{net}} = \min_{i \in S} T_i = \min_{i \in S} E_i/P_i$. Note that this definition makes the analysis tractable for many different scenarios and has been extensively used, e.g., [6]–[8]. Hence, the objective of maximizing the network lifetime is $\max T_{\text{net}} = \max(\min_{i \in S} T_i)$. Equivalently, the maximization objective can be reformulated as a minimization objective, i.e., $\min -T_{\text{net}} = \min -(\min_{i \in S} T_i)$.

On the other hand, the key issue for video transmission is how to improve the video quality reconstructed at the destination. It implies that we should minimize the end-to-end video distortion at all sink nodes, i.e., $\min \sum_{i \in S} D_i = \min \sum_{i \in S}(D_i^c + D_i^t)$. Note that, by using the proposed error control scheme, nearly all the coded packets from the source are expected to be successfully recovered at the sink. Therefore, transmission distortion is negligible, and we have $\min \sum_{i \in S} D_i^c$.

According to the foregoing analysis, maximizing the network lifetime and minimizing the total video distortion can both be formulated as constrained minimization problems. Hence, the tradeoff between them can be formulated as a multiobjective programming problem. A simple and efficient way to achieve the desired tradeoff is the weighting method [26]. That is, we introduce a weighted system parameter $\alpha \in [0,1]$ and combine these two objective functions together into a single objective function, i.e., $\min\{\alpha \sum_{i \in S} D_i^c + (1-\alpha)[-(\min_{i \in S} T_i)]\}$. With the previously introduced constraints, the balance problem can be formulated as follows:

$$
\mathbf{P1}: \quad \min\left\{ \alpha \sum_{i \in S} D_i^c - (1-\alpha) \min_{i \in S} T_i \right\} \quad (13)
$$

s.t.

1) $\sum_{m \in J(s)} x^{sm} \geq R_s \; \forall s \in S$;
2) $\kappa \sum_{m \in J(s)} H_{ij}^{sm} \cdot x^{sm} = (1-p_{ij}) \cdot f_{ij}^s \; \forall(i,j) \in E \; \forall s \in S$;
3) $\sum_{s \in S} f_{ij}^s + \sum_{s \in S} \sum_{(p,q) \in \Psi(i,j)} f_{pq}^s \leq C \; \forall(i,j) \in E$;
4) $T_i = E_i/P_i \; \forall i \in S$;
5) $\sigma^2 e^{-\gamma \cdot R_i \cdot (P_i^c)^{2/3}} \leq D_i^c \; \forall i \in S$

where x^{sm}, f_{ij}^s, T_i, R_i, and D_i^c are the nonnegative optimization variables, and x^{sm} is the allocated rate on the mth path of sensor node s.

Constraint 2 shows that f_{ij}^s is a dummy variable that can be expressed by the functions of x^{sm}, i.e., $f_{ij}^s = \sum_{m \in J(s)} \eta_{ij} \cdot H_{ij}^{sm} x^{sm}$, where we let $\eta_{ij} \triangleq \kappa/(1-p_{ij})$ to simplify the expression. Constraint 4 is not convex and usually hard to solve in practice. Therefore, we introduce a new variable $t_i = 1/T_i$ and make an equivalent transformation of $E_i t_i = P_i$. Note that t_i can be interpreted as node i's normalized power consumption with respect to its initial energy budget E_i. Namely, $\max(\min_{i \in S} T_i) = \min(\max_{i \in S} t_i)$. As for Constraint 5, we simplify it by a logarithmic transformation $\log(\sigma^2/D_i^c) = \gamma \cdot (P_i^c)^{2/3} \cdot R_i$.

In the objective function, the maximum function $\max_{i \in S} t_i$ is not differentiable and is difficult to solve in a distributed manner. Following the same analysis in [2], we can obtain

$$
\max_{i \in S} t_i = \|t\|_\infty \approx \|t\|_k = \left(\sum_{i \in S} t_i^k \right)^{1/k}. \quad (14)
$$

It can be verified that $\|t\|_k$ uniformly converges to $\|t\|_\infty$ at a large k. See also in Section IV-D.

In addition, in a reasonable way, we slightly rewrite the objective function $\|t\|_k$ to $\|t\|_k^k$, and Problem $\mathbf{P1}$ can be rewritten as

$$
\mathbf{P2}: \quad \min \alpha' \sum_{i \in S} D_i^c + (1-\alpha') \sum_{i \in S} t_i^k \quad (15)
$$

s.t.

1) $\sum_{m \in J(s)} x^{sm} \geq R_s \ \forall s \in S$;
2) $\sum_{s \in S} \sum_{(p,q) \in \Psi(i,j)} \sum_{m \in J(s)} \eta_{pq} \cdot H_{pq}^{sm} x^{sm}$
   $+ \sum_{s \in S} \sum_{m \in J(s)} \eta_{ij} \cdot H_{ij}^{sm} x^{sm} \leq C \ \forall (i,j) \in E$;
3) $E_i t_i = P_i^c + \sum_{s \in S} \sum_{j:(i,j) \in E} \sum_{m \in J(s)} \eta_{ij} \epsilon_{ij} \cdot H_{ij}^{sm} x^{sm}$
   $+ \sum_{s \in S} \sum_{j:(j,i) \in E} \sum_{m \in J(s)} (\eta_{ji} \xi \cdot H_{ji}^{sm} x^{sm}$
   $+ \varphi \cdot H_{ji}^{sm} x^{sm}) \ \forall i \in S$;
4) $(1/\gamma R_i) \log(\sigma^2/D_i^c) \leq (P_i^c)^{2/3} \ \forall i \in S$

where x^{sm}, t_i, R_i, and D_i^c are the optimization variables.

B. Distributed Algorithm

To solve Problem **P2** in a distributed manner, we use the primal decomposition approach [27] and propose a two-level optimization procedure, i.e.,

$$\mathbf{P2a}: \quad \min \alpha' \sum_i D_i^c + (1-\alpha') \sum_i t_i^k \quad (16)$$

s.t.

1) $\sum_{m \in J(s)} x^{sm} \geq R_s \ \forall s \in S$;
2) $\sum_s \sum_m \eta_{ij} \cdot H_{ij}^{sm} x^{sm} + \sum_{s \in S} \sum_{(p,q)} \sum_m \eta_{pq}$
   $\cdot H_{pq}^{sm} x^{sm} \leq C \ \forall (i,j) \in E$;
3) $E_i t_i = P_i^c + \sum_s \sum_{j:(i,j)} \sum_m \eta_{ij} \epsilon_{ij} \cdot H_{ij}^{sm} x^{sm} +$
   $\sum_s \sum_{j:(j,i)} \sum_m (\eta_{ji} \xi \cdot H_{ji}^{sm} x^{sm} + \varphi \cdot H_{ji}^{sm} x^{sm}) \ \forall i \in S$;
4) $(1/\gamma R_i) \log(\sigma^2/D_i^c) \leq (P_i^c)^{2/3} \ \forall i \in S$.

$$\mathbf{P2b}: \quad \min U^*(\mathbf{R}) \quad \text{s.t.} \quad R_i \geq 0 \quad \forall i \in S. \quad (17)$$

Problem **P2a** performs channel adaptation by allocating appropriate network resource (i.e., transmission rate and power budget) to video sessions such that they can be accommodated by the wireless channel. Problem **P2b** performs source adaptation to channel conditions and sensor states by adjusting the source coding rate on the basis of resource allocation results in Problem **P2a**. Problem **P2a** is a low-level optimization, which achieves the optimal solution under the condition that **R** is fixed. Problem **P2b** is a high-level optimization that is responsible for updating the coupling variable **R**. The objective value of the low-level optimization is locally optimal. It approximates to the global optimality using the result of the high-level optimization.

1) Low-Level Optimization (Channel Adaptation): To solve the low-level optimization, we relax constraints 1, 2, and 4, and formulate the following Lagrangian [28]:

$$\mathbf{L}(\lambda, \upsilon, \mu, \mathbf{x}, \mathbf{D}, \mathbf{t})$$
$$= \alpha' \sum_i D_i^c + (1-\alpha') \sum_i t_i^k$$
$$+ \sum_s \lambda_s \left(-\sum_m x^{sm} + R_s \right)$$
$$+ \sum_{(i,j)} \upsilon_{ij} \left(\sum_s \sum_m \eta_{ij} \cdot H_{ij}^{sm} x^{sm} \right.$$

$$\left. + \sum_s \sum_{(p,q)} \sum_m \eta_{pq} \cdot H_{pq}^{sm} x^{sm} - C \right)$$
$$+ \sum_i \mu_i \left(\frac{1}{\gamma R_i} \log \left(\frac{\sigma^2}{D_i^c} \right) - (P_i^c)^{\frac{2}{3}} \right) \quad (18)$$

where λ, υ, and μ are Lagrange multipliers. In addition, the corresponding Lagrange dual function is

$$g(\lambda, \upsilon, \mu) = \inf_{\mathbf{x}, \mathbf{D}, \mathbf{t}} \mathbf{L}(\lambda, \upsilon, \mu, \mathbf{x}, \mathbf{D}, \mathbf{t})$$

s.t.

$$E_i t_i = P_i^c + \sum_s \sum_{j:(i,j)} \sum_m \eta_{ij} \epsilon_{ij} \cdot H_{ij}^{sm} x^{sm}$$
$$+ \sum_s \sum_{j:(j,i)} \sum_m (\eta_{ji} \xi \cdot H_{ji}^{sm} x^{sm} + \varphi \cdot H_{ji}^{sm} x^{sm}). \quad (19)$$

The Lagrange dual problem of **P2a** is then defined as

$$\max \quad g(\lambda, \upsilon, \mu). \quad (20)$$

The corresponding Lagrange multiplier problem can be solved with the subgradient method as

$$\lambda_s(n+1) = \left[\lambda_s(n) + \tau(n) \left(-\sum_m x^{sm} + R_s \right) \right]^+ \quad (21)$$

$$\upsilon_{ij}(n+1) = \left[\upsilon_{ij}(n) + \tau(n) \left(\sum_{s \in S} \sum_{m \in J(s)} \eta_{ij} \cdot H_{ij}^{sm} x^{sm} \right. \right.$$
$$\left. \left. + \sum_s \sum_{(p,q)} \sum_m \eta_{pq} \cdot H_{pq}^{sm} x^{sm} - C \right) \right]^+ \quad (22)$$

$$\mu_i(n+1) = \left[\mu_i(n) + \tau(n) \left(\frac{1}{\gamma R_i} \log \left(\frac{\sigma^2}{D_i^c} \right) - (P_i^c)^{\frac{2}{3}} \right) \right]^+ \quad (23)$$

where $[\cdot]^+$ denotes the projection onto the set of nonnegative real numbers, and $\tau(n)$ is a positive step size.

In addition, the channel adaptation problem [see (16)] can further be decomposed into three separate subproblems, i.e.,

$$\mathbf{P2a-1} \quad \min \sum_s \lambda_s \left(-\sum_{m \in J(s)} x^{sm} + R_s \right)$$
$$+ \sum_{(i,j)} \upsilon_{ij} \left(\sum_{s \in S} \sum_{m \in J(s)} \eta_{ij} \cdot H_{ij}^{sm} x^{sm} \right.$$
$$\left. + \sum_{s \in S} \sum_{(p,q) \in \Psi(i,j)} \sum_{m \in J(s)} \eta_{pq} \cdot H_{pq}^{sm} x^{sm} - C \right) \quad (24)$$

$$\mathbf{P2a-2} \quad \min \alpha' \sum_i D_i^c + \sum_i \mu_i \cdot \frac{1}{\gamma R_i} \log\left(\frac{\sigma^2}{D_i^c}\right) \qquad (25)$$

$$\mathbf{P2a-3} \quad \min(1-\alpha') \sum_i t_i^k - \sum_i \mu_i \cdot (P_i^c)^{\frac{2}{3}} \qquad (26)$$

s.t.

$$E_i t_i = P_i^c + \sum_s \sum_{j:(i,j)} \sum_m \eta_{ij}\epsilon_{ij} \cdot H_{ij}^{sm} x^{sm}$$
$$+ \sum_s \sum_{j:(j,i)} \sum_m \left(\eta_{ji}\xi \cdot H_{ji}^{sm} x^{sm} + \varphi \cdot H_{ji}^{sm} x^{sm}\right).$$

Fig. 4.   Schematic diagram of joint source/channel adaptation scheme.

Subproblem **P2a − 1** is a rate control problem, in which both the rate allocation at the transport layer and the channel interference at the MAC layer are involved. **P2a − 2** aims to control and minimize the video distortion. **P2a − 3** keeps an energy conservation in wireless sensor networks. These three problems are solved separately and coordinated by Lagrange multipliers λ, υ, and μ.

Rate control problem: **P2a − 1** is similar to the classical rate control problem in wired networks [29], but it takes into account the wireless channel interference. **P2a − 1** is an unconstrained convex problem, in which the objective function is still not strictly convex. Thus, we use the subgradient method and have

$$x^{sm}(n+1) = [x^{sm}(n) - \dot{x}^{sm}]^+$$
$$= \left[x^{sm}(n) - \tau(n)\frac{\partial \mathbf{L}(\lambda,\upsilon,\mu,\mathbf{x},\mathbf{D},\mathbf{t})}{\partial x^{sm}}\right]^+. \quad (27)$$

The derivative of x^{sm} is given by

$$\dot{x}^{sm} = \tau(n)\left(-\lambda_s + \sum_{(i,j)} \upsilon_{ij} \cdot \eta_{ij} \cdot H_{ij}^{sm}\right.$$
$$\left. + \sum_{(i,j)} \sum_{(p,q)\in\Psi(i,j)} \upsilon_{ij} \cdot \eta_{pq} \cdot H_{pq}^{sm}\right). \quad (28)$$

In this case, rate control is mainly performed by the update of x^{sm}, where υ_{ij} can be viewed as the congestion price at link (i,j). For each link (i,j), if the total demand $\sum_s \sum_m \eta_{ij} \cdot H_{ij}^{sm} x^{sm} + \sum_s \sum_{(p,q)} \sum_m \eta_{pq} \cdot H_{pq}^{sm} x^{sm}$ exceeds the supply C, namely, the capacity of wireless shared medium is not sufficient to support current data flows traveling within a cluster, then the price υ_{ij} will rise to reduce the allocated rate x^{sm} and the transmission rate at link (i,j). Otherwise, υ_{ij} will decrease to attract more flows to occupy the free bandwidth.

Distortion control problem: The objective function of **P2a − 2** is still not strictly convex. Using the same subgradient algorithm, the minimum video distortion can be obtained by

$$D_i^c(n+1) = \left[D_i^c(n) - \tau(n)\left(\alpha' - \frac{\mu_i}{\gamma R_i}\frac{1}{D_i^c(n)}\right)\right]^+. \quad (29)$$
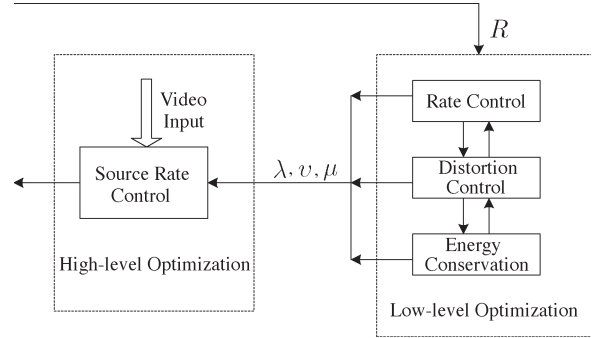
Energy conservation problem: Again, the variable t_i in **P2a − 3** can be solved using the subgradient algorithm as

$$t_i(n+1) = \left[t_i(n) - \tau(n)\left((1-\alpha')kt_i^{k-1} - \frac{2}{3}\mu_i E_i (P_i^c)^{-\frac{1}{3}}\right)\right]^+ \quad (30)$$

where we have

$$P_i^c = E_i t_i - \sum_s \sum_{j:(i,j)} \sum_m \eta_{ij}\epsilon_{ij} \cdot H_{ij}^{sm} x^{sm}$$
$$- \sum_s \sum_{j:(j,i)} \sum_m \left(\eta_{ji}\xi \cdot H_{ji}^{sm} x^{sm} + \varphi \cdot H_{ji}^{sm} x^{sm}\right). \quad (31)$$

The energy conservation at each sensor i is achieved by adjusting the value of x^{sm} and t_i, with μ_i working as the energy consumption price. If the total energy utilized at node i exceeds the current energy budget, then μ_i will rise. As a response, the communication rate x^{sm} will slow down to save the energy. Meanwhile, the normalized power consumption t_i will rise, signaling the reduction of the lifetime. Otherwise, the opposite changes will happen.

2) High-Level Optimization (Source Adaptation): We now discuss how to adapt source rate $\mathbf{R}$ in the high-level optimization to the channel conditions. As previously mentioned, the objective function $U^*(\mathbf{R})$ in **P2b** is the optimal value of **P2a** for the given $\mathbf{R}$. In addition, the high-level optimization is iteratively executed to update the value of $\mathbf{R}$. For an initial source rate R_i at sensor node i, the optimal value of **P2** is a function of R_i that can be resolved by

$$\min_{R_i \geq 0} U^*(R_i). \qquad (32)$$

Unlike the fixed source rate mechanism, the video sensor in our design can achieve the source adaptation by independently solving a localized optimization problem [see (32)], where the instantaneous source rate R_i can vary with the congestion price υ_{ij}, energy consumption price μ_i, and λ_i that are obtained from channel adaptation, as shown in Fig. 4. The integration of channel adaptation (network resource allocation) with source adaptation (source rate optimization) finally leads to an optimal performance on network lifetime and video quality.

C. Implementation Problem

A decentralized implementation of the proposed two-level iterative algorithm is summarized in Algorithm 1. For each sensor s, its path set $J(s)$ to the sink is generated at the initialization phase of the optimization procedure. Precisely, in the initialization phase, using the multipath routing protocol, each sensor s finds a set of paths $J(s)$ to the sink. In turn, the sensor s sends a message containing the value of H_{ij}^{sm} to each link. For any link (i, j) included in the mth path of node s, it has $H_{ij}^{sm} = 1$, or else, $H_{ij}^{sm} = 0$.

Algorithm 1 Distributed two-level optimization algorithm

Initialization
Set $n = 0$, $n' = 0$, and $x^{sm}(0)$, $t_s(0)$, $R_s(0)$, $D_s^c(0)$, $\lambda_s(0)$, $v_{ij}(0)$, $\mu_s(0)$ to some nonnegative value for all i, j, s, m.
repeat
    Updating at link (i, j) **in low-level implementation**:
        Receives $x^{sm}(n)$ from sensor nodes $\{s \in S | H_{ij}^{sm} = 1$ or $H_{pq}^{sm} = 1, (p, q) \in \Psi(i, j)\}$;
        Fetches $v_{ij}(n)$ stored in the local processor;
        Updates congestion price $v_{ij}(n)$ by Eq. (22);
        Sends new price $v_{ij}(n+1)$ to sensor nodes $\{s \in S | H_{ij}^{sm} = 1$ or $H_{pq}^{sm} = 1, (p, q) \in \Psi(i, j)\}$.
    Updating at sensor node s **in low-level implementation**:
        Receives the congestion price $v_{ij}(n)$ from links $\{(i, j) \in E | H_{ij}^{sm} = 1$ or $H_{pq}^{sm} = 1, (p, q) \in \Psi(i, j)\}$;
        Fetches $\lambda_s(n)$ and $\mu_s(n)$ stored in the local processor;
        Updates $x^{sm}(n)$, $D_s^c(n)$ and $t_s(n)$ by Eq. (27), (29), and (30);
        Updates $\lambda_s(n)$ and energy price $\mu_s(n)$ by Eq. (21) and (23);
        Sends new rate $x^{sm}(n+1)$ to links $\{(i, j) \in E | H_{ij}^{sm} = 1$ or $H_{pq}^{sm} = 1, (p, q) \in \Psi(i, j)\}$.
    Updating at source node s **in high-level implementation**:
        Sensor s adjusts source rate $R_s(n')$ according to Eq. (32).
until All variables converge to the optimums.

Within the implementation of network coding, practical random network coding [22] is used to distribute the source packets of multiple generations. Here, we assume that intrasession network coding [30] is implemented within each unicast session to ensure easy operation. During data transmission, each video sensor combines its received packets of the same generation of the same source node from different upstream links. To cope with asynchronous transmission, we use the buffer model [22] to synchronize the packet arrival and departure. In the buffer model of relay nodes, packets that arrive at a node on any of the incoming links are put into a single buffer sorted by the generation number and the source node number. Subsequently, whenever there is a transmission opportunity at an outgoing link, the number of packets of every source node's every generation in the buffer is checked, and a packet is generated containing a random linear combination of all the packets that belong to the generation with the largest number of packets. After the generated packet is transmitted to the outgoing link,
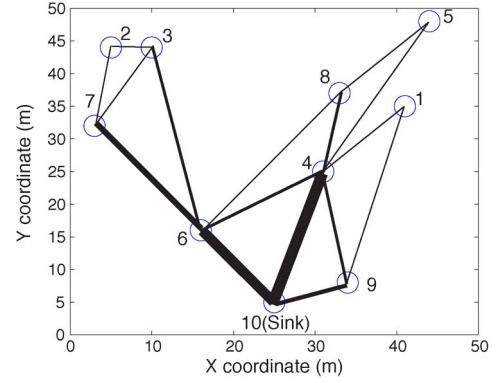

Fig. 5. Topology of the WVSN with the illustration of aggregate link rates.

TABLE I
CONFIGURATION OF MODEL PARAMETERS IN WVSN

Para.	Description	Value
σ^2	Average input variance of video sequence (MSE)	3500
γ	Equivalent encoding efficiency coefficient	$5W^{\frac{2}{3}}/Mbps$
ϵ_{ij}	Transmission energy cost of link (ij)	$0.2J/Mb$
ξ	Energy consumption cost of the radio receiver	$0.1J/Mb$
q	Galois Field size	8
h	Generation size	50
φ	Power consumption cost of network coding	$0.2J/Mb$
κ	Slack factor	1.1
p_{ij}	Packet loss rate at link (i, j)	0.1
C	Capacity of the wireless shared-medium	$5Mbps$
E_i	Initial power of sensor node i	$1MJ$
α'	Weighted system parameter	2.0×10^{-47}
Δ	Interference range	0

certain old packets are flushed from the buffer according to the flushing policy.

D. Convergence Analysis

It is straightforward to see that the two-level optimization problem has a unique solution following the foregoing distributed procedures. A formal proof of the convergence directly follows from the properties of the decomposition principle [27] and is omitted in this paper. In addition, the solution of Problem **P2** provides a lower bound to approximate the optimal solution of **P1** with respect to the normalized power consumption $\mathbf{t}$.

Proposition 1: Letting $\hat{\mathbf{t}}$ and $\mathbf{t}^{(k)}$ denote the optimal normalized power consumption corresponding to Problems **P1** and **P2**, respectively, we have

$$\|\hat{\mathbf{t}}\|_\infty \leq \left\|\hat{\mathbf{t}}^{(k)}\right\|_\infty \leq |S|^{\frac{1}{k}} \cdot \|\hat{\mathbf{t}}\|_\infty$$

where $|S|$ is the number of sensor nodes in the WVSN.

The proof can be followed with a similar analysis in [2]. As $k \to \infty$, we have $|S|^{1/k} \to 1$ and $\|\hat{\mathbf{t}}^{(k)}\|_\infty \to \|\hat{\mathbf{t}}\|_\infty$. It implies that the bound provided by **P2** is very tight with respect to **P1** at a sufficiently large k.

In general, either constant step sizes or diminishing step sizes can be used for a subgradient algorithm [28]. A constant step size is more convenient for distributed implementation, whereas the corresponding subgradient algorithm will only converge to some suboptimal solution within any given small neighborhood around the optimum [27]. Using a diminishing step size, the
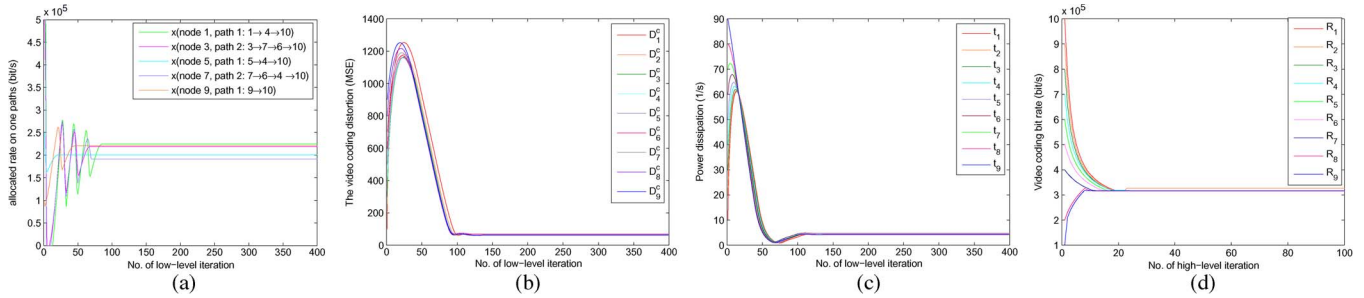
Fig. 6. Convergence behavior of the proposed distributed algorithm, where (a), (b), and (c) show the low-level iterations of variables $\mathbf{x}$, $\mathbf{D}$, and $\mathbf{t}$, respectively, and (d) illustrates the high-level iteration of the coupling variable $\mathbf{R}$.

convergence to the optimum can be guaranteed. Accordingly, we have the following result.

Proposition 2: If the step size $\tau(n)$ satisfies

$$\lim_{n \to \infty} \tau(n) = 0, \quad \sum_{n=0}^{\infty} \tau(n) = \infty$$

then for the sequence $\{\mathbf{t}^{(k)}(n)\}$ generated by the iterative algorithm given in (30), we have

$$\lim_{n,k \to \infty} \left\| \mathbf{t}^{(k)}(n) - \hat{\mathbf{t}} \right\| = 0.$$

V. SIMULATION RESULTS

In this section, we present simulation results to demonstrate the performance of the proposed distributed algorithm. We consider a static WVSN with ten nodes randomly distributed in a square region of 50 m × 50 m, as illustrated in Fig. 5, where node 10 is set to the sink, and the other nodes are video sensors. Each sensor has a maximum transmission range of 30 m. For every sensor node, we find two shortest paths to the sink, and all nine sensors encode the videos and transmit them to the sink through multiple paths. Numerically, the values of all the related model parameters are tentatively listed in Table I.

In Fig. 5, we also depict the aggregate link rates solved by the proposed distributed algorithm for the set of links E. The thickness of an edge is proportional to the amount of aggregate flow at the corresponding link. The traffic generated from all sensors is transported by the random network coding scheme via multiple paths helping reduce the transmission distortion.

A. Convergence Behavior of the Proposed Algorithm

The convergence results of both low-level and high-level optimization iterations are shown in Fig. 6. In accordance with the three low-level subproblems $\mathbf{P2a} - \mathbf{1} \sim \mathbf{P2a} - \mathbf{3}$, Fig. 6(a)–(c) shows the convergence behavior of the corresponding optimization variables $\mathbf{x}$, $\mathbf{D}$, and $\mathbf{t}$ during the low-level optimization update at a fixed step size of 0.01. Here, we set $k = 10$ and $\alpha' = 2.0 \times 10^{-47}$ in the optimization objective. Specifically, Fig. 6(a) illustrates the low-level iteration of allocated rates on the sensors' paths, and the convergence of the video distortion and the power dissipation $(1/T_i)$ at each sensor node is shown in Fig. 6(b) and (c). It can be seen that all these three types of optimization variables can achieve optimal values after about 100 iterations.

The convergence behavior of high-level optimization is shown in Fig. 6(d), where we present the coupling variable $\mathbf{R}$ for illustration. We can observe that the video encoding bit rate $\mathbf{R_i}$ for each sensor can quickly converge to its optimal value after 20 iterations. Based on the performance of both low- and high-level optimizations, it can be seen that the proposed algorithm can quickly converge to a steady state after a relatively short period of time.

B. Tradeoff Between Video Distortion and Network Lifetime

The impact of weighted system parameter α' on the tradeoff between the total video distortion minimization and the network lifetime maximization is illustrated in Fig. 7. Fig. 7(a) and (b) illustrates the impact of the weighted system parameter α' on the average video distortion and the network lifetime. We can observe that as the weighted system parameter α' decreases, the corresponding optimal network lifetime increases with the increment of the video distortion. On the contrary, the network lifetime decreases and the average video distortion decreases as the increment of α'. Fig. 7(c) shows the tradeoff between the average video distortion and the network lifetime when α' varies. We can observe that when α' reduces to an extremely small value, e.g., $\alpha' = 3.0 \times 10^{-48}$, the network lifetime approximately achieves its maximal value, since at this time the network lifetime maximization problem is the dominant problem, which can approximate the original optimization problem. For the same reason, when α' increases to an relatively large value, e.g., $\alpha' = 6.0 \times 10^{-47}$, the original optimization problem transforms to the total distortion minimization problem.

C. Comparison of NC With RSE

Fig. 8 compares the simulation results solved by the proposed algorithm with NC and the algorithm with typical link-by-link RSE coding scheme [8] under different configurations of energy consumption model parameters. In the first case, the network coding power consumption cost is set to 0.12 J/Mb, whereas the RSE encoding and decoding power consumption cost are set to 0.08 and 0.21 J/Mb [8]. It can be seen that the algorithm with network coding only slightly outperforms that with RSE error control scheme. The reason is that under this parameter configuration, the power consumption of both network coding and the RSE scheme is quite small in comparison with the video coding power consumption and, thus, takes up a minor
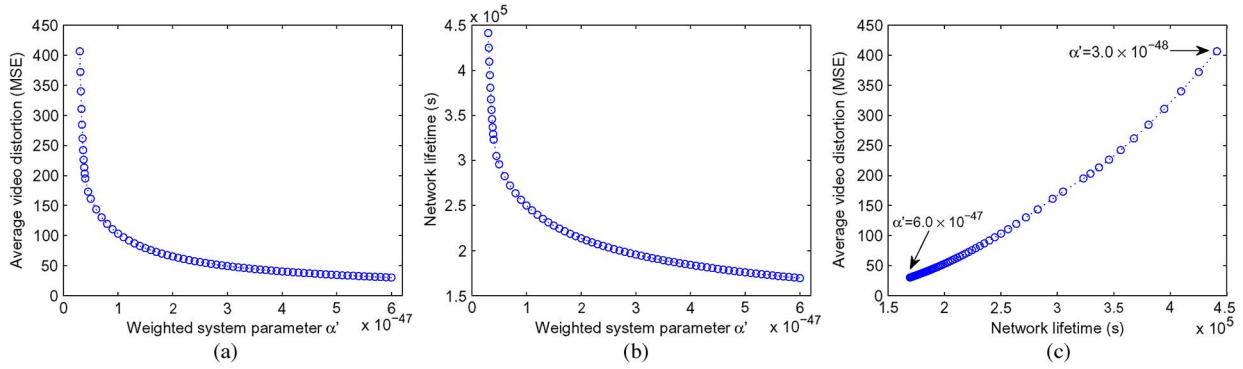
Fig. 7. Impact of weighted system parameter α' on (a) the average video distortion, (b) the network lifetime, and (c) the tradeoff between the average video distortion and the network lifetime.
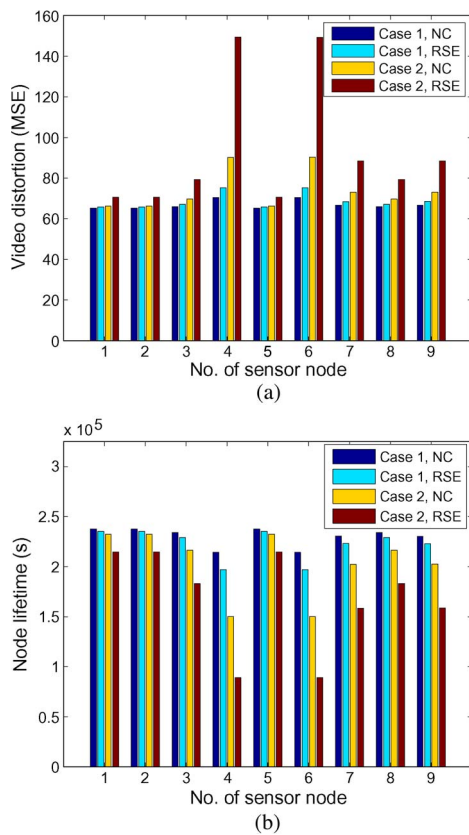

Fig. 8. Comparison of (a) the video distortion and (b) the lifetime at each sensor node.

Fig. 9. Simulation results under different source rate R_i. (a) Average video distortion and (b) network lifetime.

part of the entire node power consumption. To more explicitly show the difference of simulation results, in the second case, we enlarge the network coding power consumption cost to 1.2 J/Mb, and accordingly, the encoding and decoding power consumption costs of RSE are extended to 0.8 and 2.1 J/Mb. Here, we observe that network coding performs better than the RSE scheme with both lower video distortion and longer node lifetime for each sensor node.

D. Impact of Source Rate Adaptation

In this section, we compare the performance achieved by source rate adaptation of the high-level optimization and that
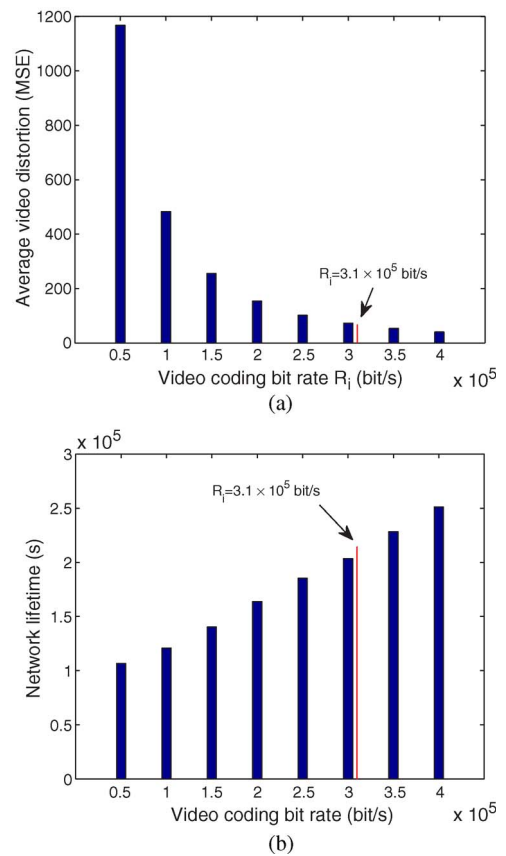
with fixed source rate $\mathbf{R}$ (i.e., where the high-level optimization is negligible). For each sensor node i, the fixed source rate R_i varies from 50 to 400 kb/s, and the results of average video distortion and network lifetime are shown in Fig. 9. Utilizing the proposed algorithm with both low- and high-level iterations, the optimal average video distortion and network lifetime can be obtained when the source rate is 310 kb/s, which are accordingly marked by a red line in both Fig. 9(a) and (b), respectively. Fig. 9 can also be interpreted in another way as the illustration of high-level convergence, i.e., when the proposed algorithm initially starts from either side of (to the left or to the right of) 310 kb/s, it will converge (rightward or leftward)
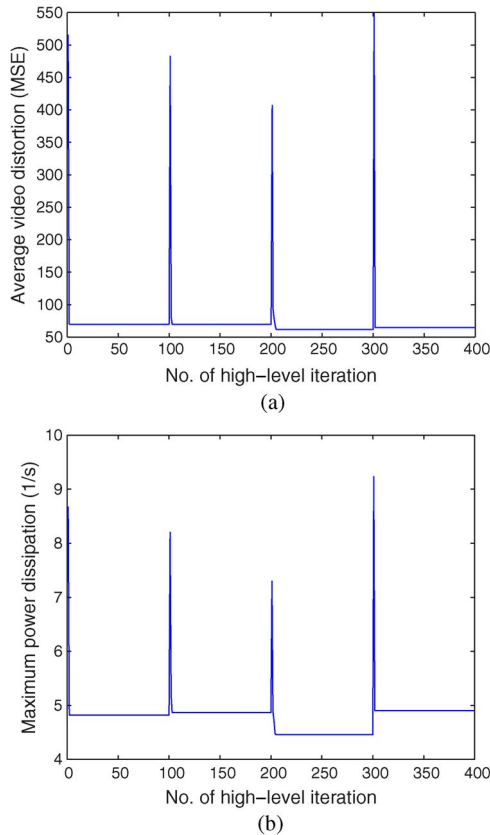
Fig. 10.   Convergence behavior of the proposed algorithms when network fluctuation occurs. (a) Average video distortion and (b) the maximum power dissipation, i.e., $1/T_{\text{net}}$.

to the global optimality when the source rate in high-level iteration ends up with $R_i = 310$ kb/s. Although both average video distortion and network lifetime are better when the fixed source rate is larger than 310 kb/s, it cannot be achieved since at this time, the wireless network channel interference constraint is violated.

E. Impact of Dynamic Network Change

We study the convergence behavior of the proposed distributed algorithm under the dynamic change of the video content and network topology, and the results are shown in Fig. 10. We characterize the video content with the average input variance σ^2. Initially, the optimization iteration begins with $\sigma^2 = 4000$. At iteration 100, nodes 8 and 9 leave the network, and the average input variance is reduced to 3500. Meanwhile, both the average video distortion and the maximum power dissipation among all sensor nodes $(1/T_{\text{net}})$ adapt themselves to this change and quickly converge to another steady state after about five iterations. At iteration 200, nodes 8 and 9 rejoin the network, and σ^2 is varied from 3500 to 2500. The values of the average video distortion and the maximum power dissipation transit from the previous steady state to a new steady state after about ten iterations. At iteration 300, node 9 leaves the network again, and σ^2 increases to 4500. Similarly, the values of the average video distortion and the maximum power dissipation converge from the previous steady state to a new steady state after about five iterations.
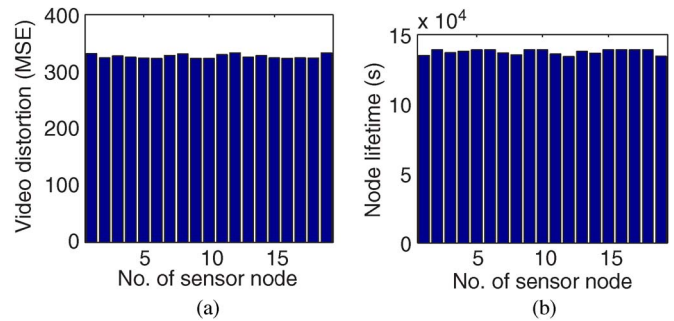

Fig. 11.   Simulation results for each sensor node in random network with 20 nodes. (a) Video distortion and (b) the node lifetime.
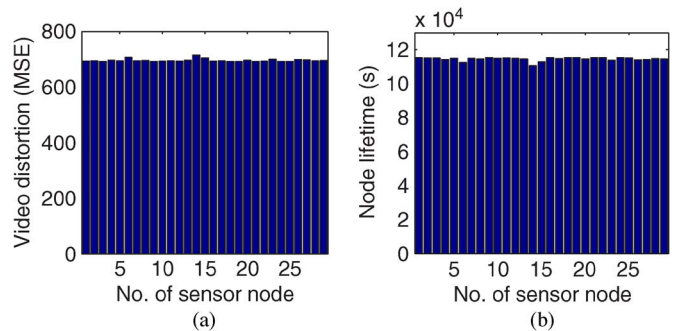

Fig. 12.   Simulation results for each sensor node in random network with 30 nodes. (a) Video distortion and (b) the node lifetime.

In conclusion, the results in Fig. 10 demonstrate that the proposed distributed algorithm can quickly reconverge to a steady state under dynamic change of network conditions.

F. Impact of Network Scale

To evaluate the impact of network scale, we vary the size of the networks and accordingly implement the proposed algorithm on two larger networks, where 20 and 30 nodes are randomly located in the square regions of 80 m × 80 m and 100 m × 100 m, respectively. With regard to the video distortion and lifetime of each node, Figs. 11 and 12 show the simulation results on the two network topologies. In addition, we compare the simulation results of the proposed algorithm on different network scales, and the comparison of the achieved average video distortion and network lifetime is shown in Fig. 13(a) and (b). We observe that as the scale of the network increases, the duty of data relaying at each sensor node becomes heavier, and thus relay nodes will consume higher power in the transmission, reception, and network coding, which results in the worse network performance with higher average video distortion and shorter network lifetime.

G. Impact of Packet Loss Rate

By varying the average packet loss rate of each wireless link from 5% to 30%, the average video distortion and the network lifetime solved by the proposed algorithm are shown in Fig. 14(a) and (b), respectively. It can be seen that, as the average packet loss rate increases, the average video distortion increases, and the network lifetime decreases. The reason is
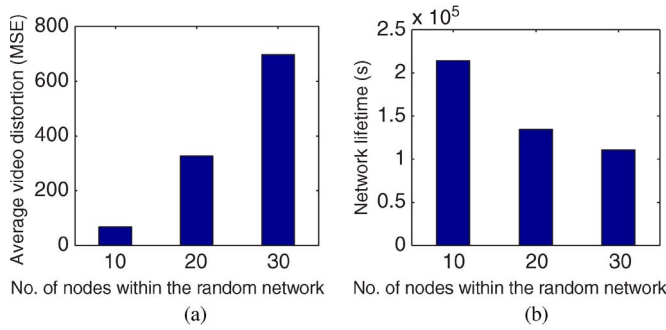
Fig. 13.   Comparison of different network scales. (a) Average video distortion and (b) the network lifetime.
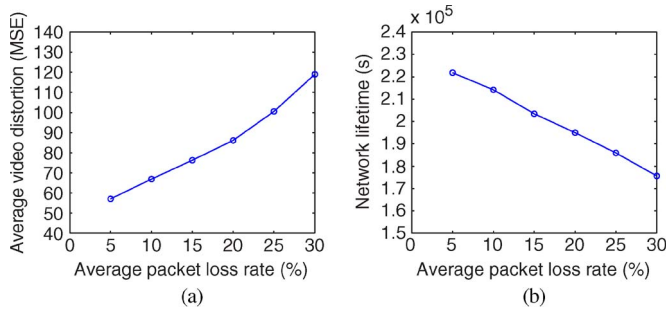

Fig. 14.   Comparison of different average packet loss rates. (a) Average video distortion and (b) the network lifetime.
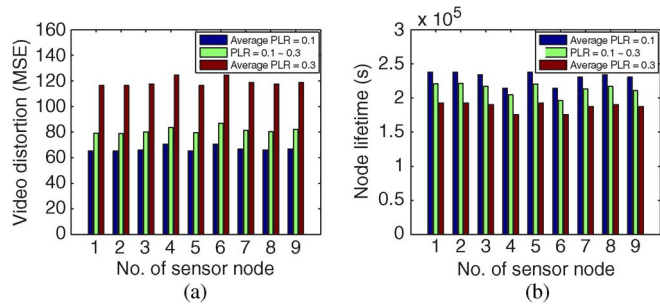

Fig. 15.   Comparison between fixed average packet loss rates and link packet loss rate proportional to its distance. (a) Video distortion and (b) the node lifetime.

as follows: For a successful decoding, the number of coded packets injected on link (i, j) (denoted by N_Y) should be sufficient to offset the packet loss rate of that link, and N_Y should satisfy $N_Y \geq h/(1 - p_{ij})$. Therefore, N_Y will increase as the increment of the average packet loss rate, which causes the worse performance of the entire network. Furthermore, we investigate the performance of the proposed algorithm when the packet loss rate of each wireless link takes into consideration the distance of that link. Assume that the packet loss rate of each link is chosen between 10% and 30% and proportional to the distance of that link. Accordingly, the video distortion and lifetime of all sensor nodes are shown in Fig. 15.
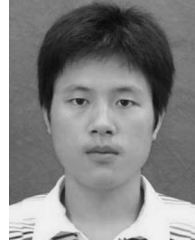
VI. CONCLUDING REMARKS

In this paper, we have investigated the performance tradeoff between maximum network lifetime and minimum video distortion for WVSNs. To increase the wireless network efficiency,

a joint source/channel rate adaptation strategy is proposed, in which the channel adaptation is responsible for network resource allocation, whereas the source adaptation is employed for source rate optimization. By jointly optimizing the video encoding rate, the transmission rate, and the integrate power consumption, we formulated this tradeoff issue as a weighted convex programming and then resolved it in a fully distributed manner by primal decomposition and Lagrange dual method. Through extensive numerical and simulation experiments, we evaluated the convergence performance of the proposed algorithm and demonstrated that the proposed algorithm can provide the best tradeoff performance in dynamic network settings and well support different network scales.

REFERENCES

[1] Z. He and D. Wu, "Resource allocation and performance analysis of wireless video sensors," *IEEE Trans. Circuits Syst. Video Technol.*, vol. 16, no. 5, pp. 590–599, May 2006.

[2] R. Madan, Z. Luo, and S. Lall, "A distributed algorithm with linear convergence for maximum lifetime routing in wireless sensor networks," in *Proc. ACCCC*, Sep. 2005, pp. 896–905.

[3] Y. Cui, Y. Xue, and K. Nahrstedt, "A utility-based distributed maximum lifetime routing algorithm for wireless networks," *IEEE Trans. Veh. Technol.*, vol. 55, no. 3, pp. 797–805, May 2006.

[4] H. Wang, Y. Yang, M. Ma, J. He, and X. Wang, "Network lifetime maximization with cross-layer design in wireless sensor networks," *IEEE Trans. Wireless Commun.*, vol. 7, no. 10, pp. 3759–3768, Oct. 2008.

[5] R. Jantti and S.-L. Kim, "Joint data rate and power allocation for lifetime maximization in interference limited ad hoc networks," *IEEE Trans. Wireless Commun.*, vol. 5, no. 5, pp. 1086–1094, May 2006.

[6] R. Madan, S. Cui, S. Lall, and A. N. Goldsmith, "Cross-layer design for lifetime maximization in interference-limited wireless sensor networks," *IEEE Trans. Wireless Commun.*, vol. 5, no. 11, pp. 3142–3152, Nov. 2006.

[7] J. Zhu, S. Chen, B. Bensaou, and K. L. Hung, "Tradeoff between lifetime and rate allocation in wireless sensor networks: A cross layer approach," in *Proc. IEEE INFOCOM*, May 2007, pp. 267–275.

[8] Y. He, I. Lee, and L. Guan, "Distributed algorithms for network lifetime maximization in wireless visual sensor networks," *IEEE Trans. Circuits Syst. Video Technol.*, vol. 19, no. 5, pp. 704–718, May 2009.

[9] Y. H. Lee and Y. B. Ness, "Power adaptation for BPSK signaling with average and peak power constraints in Rayleigh fading channels," *IEEE Trans. Commun.*, vol. 51, no. 11, pp. 1871–1876, Nov. 2003.

[10] S. T. Chung and A. J. Goldsmith, "Degrees of freedom in adaptive modulation: A unified view," *IEEE Trans. Commun.*, vol. 49, no. 9, pp. 1561–1571, Sep. 2001.

[11] D. V. Djonin, A. K. Karmokar, and V. K. Bhargava, "Joint rate and power adaptation for type-I hybrid ARQ systems over correlated fading channels under different buffer-cost constraints," *IEEE Trans. Veh. Technol.*, vol. 57, no. 1, pp. 421–435, Jan. 2008.

[12] J. C. F. Li, S. Dey, and J. Evans, "Maximal lifetime power and rate allocation for wireless sensor systems with data distortion constraints," *IEEE Trans. Signal Process.*, vol. 56, no. 5, pp. 2076–2090, May 2008.

[13] S. Choi and K. G. Shin, "A class of adaptive hybrid ARQ schemes for wireless links," *IEEE Trans. Veh. Technol.*, vol. 50, no. 3, pp. 777–790, May 2001.

[14] A. J. McAuley, "Reliable broadband communication using a burst erasure correcting code," in *Proc. ACM SIGCOMM*, Philadelphia, PA, Sep. 1990, pp. 297–306.

[15] R. Ahlswede, N. Cai, S.-Y. Li, and R. W. Yeung, "Network information flow," *IEEE Trans. Inf. Theory*, vol. 46, no. 4, pp. 1204–1216, Jul. 2000.

[16] X. Zhang and B. Li, "Optimized multi-path network coding in lossy wireless networks," in *Proc. IEEE ICDCS*, 2008, pp. 243–250.

[17] D. S. Lun, M. Mdard, R. Koetter, and M. Effros, "On coding for reliable communication over packet networks," *Phys. Commun.*, vol. 1, no. 1, pp. 3–20, Mar. 2008.

[18] Z. Guo, B. Wang, and J. Cui, "Efficient error recovery using network coding in underwater sensor networks," in *Proc. IFIP Netw.*, Atlanta, GA, May 14–18, 2007, pp. 227–238.

[19] K. Stuhlmuller, N. Farber, M. Link, and B. Girod, "Analysis of video transmission over lossy channels," *IEEE J. Sel. Areas Commun.*, vol. 18, no. 6, pp. 1012–1032, Jun. 2000.

[20] X. Zhu, E. Setton, and B. Girod, "Congestion-distortion optimized video transmission over ad hoc networks," *J. Signal Process.: Image Commun.*, vol. 20, no. 8, pp. 773–783, Sep. 2005.

[21] K. Yuen, B. Liang, and B. Li, "A distributed framework for correlated data gathering in sensor networks," *IEEE Trans. Veh. Technol.*, vol. 57, no. 1, pp. 578–593, Jan. 2008.

[22] P. A. Chou, T. Wu, and K. Jain, "Practical network coding," in *Proc. 51st Allerton Conf. Commun., Control, Comput.*, Oct. 2003, pp. 122–131.

[23] W. Lou, W. Liu, and Y. Zhang, "Performance optimization using multipath routing in mobile ad-hoc and wireless sensor networks," in *Combinatorial Optimization in Communication Networks*, M. Cheng, Y. Li, and D.-Z. Zhu, Eds.   Norwell, MA: Kluwer, 2005.

[24] S. Katti, H. Rahul, W. Hu, D. Katabi, M. Medard, and J. Crowcroft, "XORs in the air: Practical wireless network coding," in *Proc. ACM SIGCOMM*, 2006, pp. 243–254.

[25] S. Appadwedula, M. Goel, N. R. Shanbhag, D. L. Jones, and K. Ramchandran, "Total system energy minimization for wireless image transmission," *J. VLSI Signal Process. Syst.*, vol. 27, no. 1, pp. 99–117, Feb. 2001.

[26] K. Miettinen, *Nonlinear Multiobjective Optimization*.   Norwell, MA: Kluwer, 1999.

[27] D. Palomar and M. Chiang, "A tutorial on decomposition methods and distributed network resource allocation," *IEEE J. Sel. Areas Commun.*, vol. 24, no. 8, pp. 1439–1451, Aug. 2006.

[28] S. Boyd and L. Vandenberghe, *Convex Optimization*.   Cambridge, U.K.: Cambridge Univ. Press, 2004.

[29] F. P. Kelly, A. K. Maulloo, and D. K. H. Tan, "Rate control for communication networks: Shadow prices, proportional fairness and stability," *J. Oper. Res. Soc.*, vol. 49, no. 3, pp. 237–252, Mar. 1998.

[30] T. Ho and H. Viswanathan, "Dynamic algorithms for multicast with intra-session network coding," *IEEE Trans. Inf. Theory*, vol. 55, no. 2, pp. 797–815, Feb. 2009.

Junni Zou (M'07) received the M.S. and Ph.D. degrees in communication and information systems from Shanghai University, Shanghai, China, in 2004 and 2006, respectively.

Since 2006, she has been with the School of Communication and Information Engineering, Shanghai University, where she is an Associate Professor. She has published over 40 international journal/conference papers. Her research interests include distributed resource allocation, multimedia communication, and network information theory.

Dr. Zou is a member of the Technical Committee on Signal Processing of the Shanghai Institute of Electronics.

Hongkai Xiong (M'01–SM'10) received the Ph.D. degree in communication and information systems from Shanghai Jiao Tong University (SJTU), Shanghai, China, in 2003.

Since 2003, he has been with the Department of Electronic Engineering, SJTU, where he is an Associate Professor. In SJTU, he directs the "Intelligent Video Modeling" Laboratory and the "Multimedia Communication" area of the Key Laboratory of the Ministry of Education of China—"Intelligent Computing and Intelligent System," which is also cogranted by Microsoft Research. From December 2007 to December 2008, he was a Research Scholar with the Department of Electrical and Computer Engineering, Carnegie Mellon University, Pittsburgh, PA. He has published over 90 international journal/conference papers. His research interests include source coding/network information theory, signal processing, computer vision and graphics, and statistical machine learning.

Dr. Xiong was the recipient of the New Century Excellent Talents in University in 2009. In 2008, he received the Young Scholar Award from SJTU. He has served for various IEEE conferences as a Technical Program Committee member. In addition, he is a member of the Technical Committee on Signal Processing of the Shanghai Institute of Electronics.

Chenglin Li received the B.S. and M.S. degrees in electronic engineering in 2007 and 2009, respectively, from Shanghai Jiao Tong University, Shanghai, China, where he is currently working toward the Ph.D. degree.

His main research interests include network-oriented image/video processing and communication and network-based optimization for video sources.
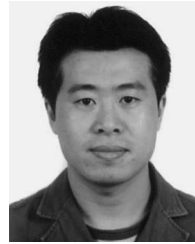
Ruifeng Zhang (S'07–M'10) received the B.S. degree in electronics engineering from Taiyuan University of Science and Technology, Taiyuan, China, in 1999, the M.S. degree in electronics engineering from Shanghai University, Shanghai, China, in 2003, and the Ph.D. degree in information from the Institute National des sciences appliques de Lyon, Lyon, France, in 2009.
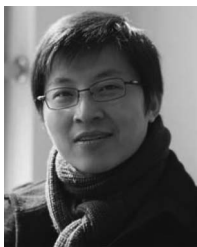
He is currently with the Key Laboratory of Special Fiber Optics and Optical Access Networks, Shanghai University. His research interests include wireless communications, cooperative opportunistic communications, wireless sensor networks, and multiple-antenna wireless communication systems and networks.

Zhihai He (S'98–M'01–SM'06) received the B.S. degree in mathematics from Beijing Normal University, Beijing, China, in 1994, the M.S. degree in mathematics from the Institute of Computational Mathematics, Chinese Academy of Sciences, Beijing, in 1997, and the Ph.D. degree in electrical engineering from the University of California, Santa Barbara, in 2001.

In 2001, he was a Member of Technical Staff with Sarnoff Corporation, Princeton, NJ. Since 2003, he has been an Assistant Professor with the Department of Electrical and Computer Engineering, University of Missouri, Columbia. His current research interests include image/video processing and compression, network transmission, wireless communication, computer vision analysis, sensor networks, and embedded system design.

Dr. He is a Member of the Visual Signal Processing and Communication Technical Committee of the IEEE Circuits and Systems Society and serves as a Technical Program Committee Member or Session Chair for a number of international conferences. He currently serves as an Associate Editor for the IEEE TRANSACTIONS ON CIRCUITS AND SYSTEMS FOR VIDEO TECHNOLOGY (TCSVT) and the *Journal of Visual Communication and Image Representation*. He is also a Guest Editor for the IEEE TCSVT Special Issue on Video Surveillance. He received the 2002 IEEE TCSVT Best Paper Award and the SPIE Visual Communications and Image Processing Young Investigator Award in 2004.